

# A planetary system with gas giants and super-Earths around the nearby M dwarf GJ 676A

## Optimizing data analysis techniques for the detection of multi-planetary systems

Guillem Anglada-Escudé<sup>1</sup>, Mikko Tuomi<sup>2,3</sup>

<sup>1</sup> Universität Göttingen, Institut für Astrophysik, Friedrich-Hund-Platz 1, 37077 Göttingen, Germany

<sup>2</sup> University of Hertfordshire, Centre for Astrophysics Research, Science and Technology Research Institute, College Lane, AL10 9AB, Hatfield, UK

<sup>3</sup> University of Turku, Tuorla Observatory, Department of Physics and Astronomy, Väisäläntie 20, FI-21500, Piikkiö, Finland

submitted March 2012

### ABSTRACT

**Context.** Several M dwarfs are targets of systematical monitoring in searches for Doppler signals caused by low mass exoplanet companions. As a result, an emergent population of high multiplicity planetary systems around low mass stars starts to show up as well.

**Aims.** We optimize classic data analysis methods and develop new ones to enhance the sensitivity towards lower amplitude planets in high multiplicity systems. We apply this methods on the public HARPS observations of GJ 676A, a nearby and relatively quiet M dwarf with one reported gas giant companion.

**Methods.** We rederive Doppler measurements from public HARPS spectra using the recently developed template matching method (HARPS-TERRA software). We use refined versions of periodograms to assess the presence of additional low mass companions. We also analyse the same dataset using Bayesian statistics tools and compare the performance of both approaches.

**Results.** We confirm the already reported massive gas giant candidate and the presence of a long period trend in the Doppler measurements. In addition to that, we find very secure evidence in favour of two new candidates in close-in orbits and masses in the super-Earth mass regime. Also, the increased time-span of the observations allows the detection of curvature in the long period trend suggesting the presence of a massive outer companion whose nature is still unclear.

**Conclusions.** Even though the increased sensitivity of our new periodogram tools, we find that Bayesian methods are significantly more sensitive and reliable in the early detection of candidate signals but more works is needed to properly quantify their robustness against false positives. While hardware development is important in increasing the Doppler precision, development of data analysis techniques can help revealing new results from existing data sets with significant less resources. These new planetary system holds the record of minimum mass range (from 4.5  $M_{\oplus}$  to 5  $M_{Jup}$ ) and period range (from 3.6 days to more than 10 years), being the first exoplanetary system with a general architecture similar to our Solar System. GJ 676A can be happily added to the family of high multiplicity planetary systems around M dwarfs.

**Key words.** techniques : radial velocities – methods : data analysis – stars: planetary systems – stars: individual :GJ 676A

## 1. Introduction

Doppler spectroscopy is currently the most effective method in detecting planet candidates orbiting nearby stars. The current precision enables the detection of planets of a few Earth masses in close-in orbits, especially around low mass stars (Mayor et al. 2009). Two methods are currently used to get precision Doppler measurements in the visible part of the spectrum : the gas cell and the stabilized spectrograph approach. The Iodine cell method consists on inserting a cell containing Iodine gas in the beam of the telescope thus providing a very accurate method to solve for the wavelength solution, instrumental profile variability and the Doppler changes in the stellar spectrum (Butler et al. 1996). The second approach is based on building a mechanically stable fiber-fed spectrograph calibrated with an emission lamp (Baranne et al. 1996). HARPS is the best example of a stabilized spectrograph in operation and it is installed at the 3.6m Telescope in La Silla-ESO observatory/Chile (Pepe et al. 2003).

The list of planets detected by HARPS is long and varied as can be seen in the 35 papers of the series *The HARPS search for southern extra-solar planets*. Instead of citing all of them, we refer the interested reader to the latest HARPS results presented in Pepe et al. (2011); Mayor et al. (2011); Bonfils et al. (2011). HARPS has demonstrated a radial velocity (RV) stability at the level of  $1 \text{ m s}^{-1}$  on time-scales of several years. Since January 2011, reduced data products derived from the HARPS Data Reduction Software (DRS) are publicly available through a dedicated webpage in ESO<sup>1</sup>. All data used in this work has been obtained from there.

The increasing demand for higher Doppler precision has motivated a significant investment in hardware development and a number of new stabilized spectrographs are currently under construction (e.g., Wilken et al. 2012). It is known, however, that the method employed by the HARPS-DRS to extract RV measurements (Cross-correlation function) is suboptimal in exploiting the Doppler information in the stellar spec-

Send offprint requests to: G. Anglada-Escudé, e-mail: guillem.anglada@gmail.com

<sup>1</sup> <http://archive.eso.org/wdb/wdb/eso/repro/form>

trum (Queloz 1995; Pepe et al. 2002), so developments in the data analysis techniques are also required to reach photon noise limited precision. We have recently developed a least-squares template matching method (HARPS-TERRA software, Anglada-Escudé & Butler 2012; Anglada-Escudé et al. 2012) that is able to derive precise RV measurements from HARPS spectra obtaining a substantial increment of precision on K and M dwarfs. In (Anglada-Escudé & Butler 2012), 34 observations on the M0 dwarf GJ 676A were used to illustrate the improvement in precision of the HARPS-TERRA measurements compared to those used in the discovery paper of the massive planet candidate GJ 676b (Forveille et al. 2011). Additional observations on this star have been recently released through the ESO archive, so we applied HARPS-TERRA to extract new RV measurements of the full set. In a quicklook analysis using classic periodogram methods, we found tentative evidence for additional planets in the system. However, these preliminary detections did not provide convincing results. Recent developments in the Bayesian analysis methods of Doppler data (e.g., Tuomi 2012) indicate that correlation between parameters seriously affect the sensitivity of periodogram based methods in the detection of additional low amplitude signals. Moreover, careful Bayesian analyses provide increased sensitivity to lower amplitude signals (Tuomi 2012) and seem to be less prone to false positives than methods based on sequential periodogram analyses of the residuals only (Tuomi 2011).

In this work, we develop and test data analysis methods for optimal detection of low-mass companions in multi-planetary systems and apply them to the HARPS-TERRA measurements of GJ 676A. In Section 2, we describe a new periodogram-based approach (recursive periodogram) and review the Bayesian analysis tools also developed to deal with multi-Keplerian fits. Section 3 reviews the stellar properties of GJ 676A, describes the observations, discusses periodicities detected in activity indices and describes the previously detected candidates (one massive gas giant and a long period trend Forveille et al. 2011). Section 4 analyses the RVs of GJ 676A using the aforementioned tools. Both methods (recursive periodograms and Bayesian analyses) agree in the detection of two additional sub-Neptune/super-Earth mass candidates in close-in orbits. We also use the opportunity to test the sensitivity of both detection methods by applying them to a subset of observations (first 50 epochs). We found that, while the recursive periodogram approach could only spot one of the signals at low confidence, a Bayesian analysis could already recover (or strongly suggest) the same 4 candidates much earlier. Finally, in Section 5 we place the unique features of the planetary system around GJ 676A in the context of the currently known population of exoplanets and provide some concluding remarks.

## 2. Data analysis methods

### 2.1. Recursive periodograms

Classic least-squares periodograms and derived methods (Scargle 1982; Cumming 2004) consist of adjusting a sine-wave (equivalent to a circular orbit) to a list of test periods and plot these periods against some measure of merit. When  $k$ -periodic signals are detected in the data, the corresponding Keplerian model is subtracted from the data and a least-squares periodogram is typically applied on the residuals to assess if there is a  $k+1$ th periodicity left. As noted by several authors (Anglada-Escudé et al. 2010; Lovis et al. 2011b; Tuomi 2012), non-obvious correlations between parameters are likely to decrease the significance of (yet undetected) low amplitude signals.

This is, as the number of the Keplerian signals in a model increases, the aliases of previously detected signals and other non-trivial correlations seriously affect the distribution of the residuals and, unless the new signal is very obvious, a periodogram on the residuals will not properly identify (even completely confuse) the next most likely periodicity left in the data.

To account for parameter correlation at the period search level, we have developed a generalized version of the classic least-squares periodogram optimized for multiplanet detection that we call *recursive periodogram*. Instead of adjusting sine-waves to the residuals only, a recursive periodogram consists on adjusting all the parameters of the already detected signals together with the signal under investigation. Even in the presence of correlations, candidate periods will show prominently as long as the new solution provides a net improvement to the previous global solution. In our approach and by analogy to previous least-squares periodograms, a circular orbit (sinusoid) is always assumed for the proposed new periodicity. When no previous planets are detected, this is equivalent to the Generalized least-squares periodogram discussed by Zechmeister et al. (2009), and is a natural generalization of the methods discussed by Cumming (2004) to multi-Keplerian solutions. The graphical representation of the periodogram is then obtained by plotting the obtained period for the new planet (X-axis) versus the F-ratio statistic obtained from the fit (Y-axis). The highest peak in this representation indicates, in a least-squares sense, the most likely periodic signal present in the data.

As any other classic least-squares periodogram method, one has to assess if adding a new signal is justified given the improvement of the fit. As proposed by Cumming (2004), we use the F-ratio statistic to quantify the improvement of the fit of the new model ( $k+1$  planets) compared to the null hypothesis ( $k$  planets). The F-ratio as a function of the test period is defined as

$$F(P) = \frac{(\chi_0^2 - \chi_P^2)/(N_{k+1} - N_k)}{\chi_P^2/(N_{obs} - N_{k+1})} \quad (1)$$

where  $N_k$  is the number of free parameters in the model with  $k$ -planets and  $N_{k+1}$  is the number of free parameters in the model including one more candidate in a circular orbit at period  $P$ . For a circular orbit, the number of additional parameters  $N_{k+1} - N_k$  is 2 (amplitude and phase of a sinusoid). Under the assumption of large  $N_{obs}$ , statistical independence of the observations, and Gaussian errors;  $F(P)$  would follow a Fisher F-distribution with  $N_{k+1} - N_k$  and  $N_{obs} - N_{k+1}$  degrees of freedom. The cumulative distribution (integral from 0 to the obtained F-ratio) is then used as the confidence level  $c$  at each  $P$  (also called single frequency confidence level). Because the period is a strongly non-linear parameter, each peak in a periodogram must be treated as an independent experiment (so-called independent frequencies). Given a dataset, the number of independent frequencies  $M$  can be approximated by  $P_{min}\Delta T$ , where  $\Delta T$  is the time baseline of the observations and  $P_{min}$  is the shortest period (largest frequency) under consideration. Given  $M$ , the analytic false alarm probability is finally derived as  $FAP = 1 - c^M$ .

Since the fully Keplerian problem is very non-linear, several iterations at each test period are necessary to ensure convergence of the solution. A typical recursive periodogram consists in testing several thousands of such solutions and, therefore, it is a time consuming task. As a result, special care has to be taken in using a robust and numerically efficient model to predict the observables required by the solving algorithms. We found that a slight modification of the parameterization given by

(Wright & Howard 2009) provided the best match to our needs. The only change we applied was using the initial mean anomaly  $M_0$  instead of the time of periastron  $T_0$  as a free parameter. These two quantities are related by  $2\pi T_0/P = -M_0$ . From this expression one can see that the replacement of  $T_0$  by  $M_0$  eliminates the non-linear coupling between  $T_0$  and  $P$ . (Wright & Howard 2009) also provides the partial derivatives of the observables (radial velocity) in a numerically efficient representation. The partial derivative of the RV with respect to  $M_0$  (instead of  $T_0$ ) is trivially obtained as minus the partial derivative of the radial velocity with respect to the mean anomaly  $E$  ( $\partial v/\partial M_0 = -\partial v/\partial E$ ). Beyond this change, the adopted model is identical to the one given in (Wright & Howard 2009) so, for the sake of brevity, we do not provide the full description here. To accelerate convergence, at each test period, we first solve for linear parameters only. Next, we use the Levenberg-Marquadt (Levenberg 1944) method to smoothly approach the  $\chi^2$  minimum and, finally, a few iterations of a straight non-linear least-squares solver (Press et al. 1992) are used to quickly converge to the final solution. Note that, although fitting for  $k$ -planets at each test period would seem a very time-consuming effort, we are implicitly assuming that the solver is already close to the  $\chi^2$  local minimum, so a relatively low number of non-linear iterations (between 20 and 50) are typically enough to reach the closest local minimum. Since all the orbits are re-adjusted and even though the method still suffers from some of the typical pitfalls of sequential Keplerian fitting (e.g., one can still get stucked on local minima), the solution at each test period always has a higher significance than a periodogram on the residuals, especially in the presence of correlations between parameters.

It is known that the assumptions required by the F-ratio tests might not be strictly satisfied by RV observations. Therefore, an empirical scheme is always desirable to better assess the FAP of a new detection. Since the recursive periodogram is a straight generalization of least-squares periodograms, we adopt the brute-force Monte Carlo method proposed by Cumming (2004) to obtain empirical estimates of the FAPs. This is, we compute recursive periodograms on synthetic datasets and count how many times spurious peaks with higher power than the signal under investigation are obtained by an unfortunate arrangement of the noise. Each Monte Carlo trial consists on : 1) taking the residuals to the model with  $k$ -planets and randomly permute them over the same observing epochs, 2) adding back the signal of the model with  $k$ -planets, 3) re-adjusting the solution with  $k$ -planets (new null hypothesis), 4) computing the recursive periodogram on this new synthetic dataset and, 5) recording the highest F-ratio in a file. The FAP will be the number of times we get an F-ratio higher than the original one divided by the number of trials.

A recursive periodogram can take a few tens of minutes depending on the number of datapoints and number of planets in the model. While this is not a serious issue while exploring one dataset, it becomes a problem when FAPs have to be empirically computed on many thousands of Monte Carlo trials. As a general rule, we accept new candidates if they show an empirical FAP lower than 1%. While this threshold is arbitrary, it guarantees that even if some of the proposed candidates are false positives, we will not seriously contaminate the current sample of  $\sim 700$  RV detected exoplanets with spurious detections. As a first saving measure and given that analytic FAPs are known to be over-optimistic, we will only compute empirical FAPs if the analytical FAP prediction is already lower than 1%. The chance of obtaining a false alarm in a trial is a Poisson process and, therefore, the uncertainty in the empirical FAP is  $\sim \sqrt{N_{\text{FAPs}}/N_{\text{trials}}}$ . Our aim is to guarantee that the empirical FAP is  $< 1\%$  at a  $4\text{-}\sigma$

level, so we designed the following strategy to minimize the the number of Monte Carlo trials. This is, we first run 1000 trials. If no false-alarms are detected, the candidate is accepted and the analytic FAP is used to provide an estimate of the real one. If the number of trials generating false alarms is between 1 and 20 (estimated FAP  $\sim 0.1\text{--}3\%$ ), we extend the number of trials to  $10^4$ . If the updated FAP is lower than 0.5%, we stop the simulations and accept the candidate. If the empirical FAP is still between 0.5 and 1.5%,  $5 \times 10^4$  trials are obtained and the derived FAP is used to decide if a candidate is accepted. While the computation time for 1000 trials in a single processor is prohibitively high, the computation of many recursive periodograms can be easily parallelized in modern multi-processor desktop computers. For the GJ 676A dataset and a (3+1)-planet model,  $10^3$  trials would take 2.3 days on one 2.0 GHz CPU. The same computation on 40 logical CPUs takes 1.4 hours allowing to obtain empirical FAP runs with  $10^4\text{--}10^5$  trials in less than a week.

## 2.2. Bayesian analysis methods

As in e.g. Tuomi (2012), the Bayesian analyses of the RVs of GJ 676A were conducted using samplings of the posterior probability densities, estimations of Bayesian evidences and the corresponding model probabilities based on these samples.

We sampled the posterior densities using the adaptive Metropolis algorithm (Haario et al. 2001), also described broadly in Tuomi (2011). Because it converges reliably and relatively rapidly to the posterior density in most situations, we performed several samplings of the parameter space of each model. Different samplings were started with different initial states to make sure that the global probability maximum of the parameter space was found for each model. If they all converged to the same solution, we could confidently conclude that the corresponding maximum was indeed the global one. This check was performed because it is possible that the Markov chains get stuck in a local maximum if it is sufficiently high and the initial state happens to be close to it. As a result, we could then reliably estimate the parameters using the maximum *a posteriori* (MAP) estimates and Bayesian credibility sets (BCSs) as uncertainty estimates (Tuomi & Kotiranta 2009).

The Bayesian evidences of each model were calculated using the one block Metropolis-Hastings (OBMH) estimate (Chib & Jeliazkov 2001). It requires a statistically representative sample from the posterior, available due to posterior samplings, and can be used to assess the evidences and the corresponding model probabilities with relatively little computational effort when determining the number of Keplerian signals in a RV data set favoured by the data (e.g. Tuomi 2011, 2012; Tuomi et al. 2011).

Using the OBMH estimates, we determined the probabilities of the models with differing numbers of Keplerian signals. However, we did not blindly choose the model with the greatest posterior probability and add it to the solution unless three detection criteria were also satisfied. We required that (1) the posterior probability of a model with  $k+1$  Keplerian signals was at least 150 times greater than that of a model with  $k$  signals (Kass & Raftery 1995; Tuomi 2011, 2012; Tuomi et al. 2011); (2) the RV amplitudes of every signal were significantly greater than zero (Tuomi 2012); (3) and that the periods of each signal were well constrained from above and below because if this was not the case, we could not tell whether the corresponding signals were indeed of Keplerian nature and periodic ones. These detection criteria have been used in Tuomi (2012) and they appear to provide reliable results in terms of the most trustworthy number

**Table 1.** Basic parameters of GJ 676A

Parameter	Value	Reference
R.A.	17 30 11.203	(a)
Dec.	-51 38 13.104	(a)
$\mu_{R.A.}^*$ [mas yr <sup>-1</sup> ]	-260.02 ± 1.34	(a)
$\mu_{Dec}$ [mas yr <sup>-1</sup> ]	-184.29 ± 0.82	(a)
Parallax [mas]	60.79 ± 1.62	(a)
$V^a$	9.585 ± 0.01	(b)
$K^b$	5.825 ± 0.03	(c)
Sp. type <sup>c</sup>	M0V	(b)
Mass [M <sub>⊙</sub> ] <sup>d</sup>	0.71 ± 0.04	(d)
Fe/H	+0.23 ± 0.10	(e)

**Notes.** (a) HIPPARCOS catalog, (van Leeuwen 2007) (b) (Koen et al. 2010) (c) 2MASS catalog, (Skrutskie et al. 2006) (d) Using (Delfosse et al. 2000) (e) Using (Johnson & Apps 2009)

of signals in a RV data set. We claim a detection of a Keplerian signal in the data if the Markov chains of several samplings converge to a solution that satisfies the criteria 1-3 above.

The prior probability densities were chosen to have the same quantitative forms as in (Tuomi 2012), in which e.g. the parameter space of the RV amplitude was limited to [0, 20] ms<sup>-1</sup>. However, because the RV data contains the obvious Keplerian signal of a massive candidate and a long-period trend reported (Forveille et al. 2011) with amplitudes clearly larger than 20 m s<sup>-1</sup>, the first two signals were allowed to explore a wider range of semi-major amplitudes, i.e., [0, 200] ms<sup>-1</sup>. Also, following (Tuomi 2012), we did not set the prior probabilities of different models equal but set them such that for models  $\mathcal{M}_k$  and  $\mathcal{M}_{k+1}$ , it holds that the prior probabilities satisfy  $P(\mathcal{M}_k) = 2P(\mathcal{M}_{k+1})$  for all values of  $k$ .

### 3. Observations, stellar activity and previous work

GJ 676 is a common proper motion pair of M dwarfs. The primary (GJ 676A) has been classified as an M0V star (Koen et al. 2010). Using the empirical relations of Delfosse et al. (2000), the 2MASS JHK photometry (Skrutskie et al. 2006) and its trigonometric parallax (van Leeuwen 2007), we derive a mass of 0.71 M<sub>⊙</sub> for GJ 676A. The star does not show strong evidence of activity nor evidence of youthness and, therefore, it is a good candidate for high precision RV studies (Forveille et al. 2011). The basic parameters of GJ 676A are given in Table 1. The fainter member of the pair (GJ 676B) has been classified as an M3V and is currently separated 50'' from A. From its HIPPARCOS parallax, this corresponds to a minimum separation of 800 AU and an orbital period longer than 20 000 years. At this separation, the maximum acceleration of GJ 676A caused by GJ 676B on our line of sight is about 0.05 m s<sup>-1</sup> yr<sup>-1</sup>.

New radial velocity measurements were obtained using the HARPS-TERRA software (Anglada-Escudé & Butler 2012) from HARPS spectra recently made public through the ESO archive. The spectra are provided extracted and wavelength calibrated by the HARPS-Data Reduction Software (DRS). Each HARPS spectrum consist of 72 echelle appertures covering the visible spectrum between 3800 and 6800 Å. The average spectral resolution is  $\lambda/\delta\lambda = 110000$  and each echelle apperture consists on 4096 extracted elements (or pixels). The set of public 75 spectra have been obtained by several programs over the years and typical exposure times vary between 300 to 900 seconds. The mean signal-to-noise ratio (SNR) at 6000 Å is 60 and, in a few cases, it can be as low as 22. Doppler measurements derived

with HARPS-TERRA are differential against a very high SNR template spectrum generated by coadding all the observations. The secular acceleration effect (Zechmeister et al. 2009) was subtracted from the RVs using the HIPPARCOS (van Leeuwen 2007) proper motion and parallax of the star.

Two sub-stellar companions were reported on the system by Forveille et al. (2011). The most prominent one is a massive gas giant candidate with a period of ~ 1060 days and a semi-major amplitude of ~ 120 m s<sup>-1</sup>. Strong evidence for a second, very long period candidate was also reported in Forveille et al. (2011) because of a strong trend detected in the residual to the 1 planet fit. Forveille et al. (2011) already noted that the magnitude of such trend (~ 8 m s<sup>-1</sup>) was too high to be explained by the gravitational pull of GJ 676B (~ 0.05 m s<sup>-1</sup>). Even after subtracting a model with one planet and a trend, Forveille et al. (2011) also noted that the RMS of the residuals was significantly higher (~ 3.6 m s<sup>-1</sup>) than the reported uncertainties (1 to 1.5 m s<sup>-1</sup>) which was suggestive of potential new candidates. Reanalysis of the 40 spectra available to Anglada-Escudé & Butler (2012) confirmed that, even with the increased precision derived using HARPS-TERRA (RMS 3.2 m s<sup>-1</sup>), the star did show a significant excess of RV variability.

In addition to the RV measurements, HARPS-TERRA also measures the CaII H+K activity index (S-index in the Mount Wilson system Baliunas et al. 1995) and collects the measurements provided by the HARPS-DRS on two of the cross-correlation function (CCF) parameters that are also sensitive to stellar activity : bisector span (or BIS), full-width at half-maximum of the CCF (or FWHM). The S-index is directly measured by HARPS-TERRA on the blaze-corrected spectra using the definitions given by Lovis et al. (2011a) and is an indirect measurement of the chromospheric emission and the average intensity of the stellar magnetic field. Because the strength of the magnetic field affects the efficiency of convection, some spurious RV signals should correlate with the variability in the S-index. BIS is a measure of the asymmetry of the average spectral line and should correlate with the RV if the observed offsets are caused by spots or plages rotating with the star (Queloz et al. 2001). The FWHM is a measure of the width of the mean spectral line and its variability is usually associated with changes in the convective patterns on the surface of a star that might also induce spurious RV offsets. Since the connection between activity and RV jitter on M dwarfs is not well understood yet (Lovis et al. 2011a), we restrict our analyses to evaluate if any of the indices has periodicities similar to the detected RV candidates.

No strong periodicities were detected on the BIS and the FWHM. However, the S-index did show a very strong signal with a period of 910 days (FAP ~ 0.01%). Although the signal has a similar period as the GJ 676Ab candidate, such coincidence was not mentioned in Forveille et al. (2011). Even if the periods are similar, two strong arguments favor the Keplerian interpretation of the candidate. First, the signal in the S-index signal is not in phase with the Doppler one. Second, Gomes da Silva et al. (2012) has shown that RV offsets correlated with the variability of the S-index (or similar spectroscopic indices) are at the level of a few m s<sup>-1</sup> level at most (GJ 676Ab's RV semi-amplitude is 120 m s<sup>-1</sup>). Therefore, we find it likely that the similarity in the periods is purely coincidental. Evidence for an activity cycle of ~ 1000 days is also supported by the analysis of the NaI-index done by Gomes da Silva et al. (2012) using almost the same set of observations.

In a preliminary analysis of the new 75 RVs, periodograms on the residuals to the two Keplerian solution (gas giant + trend) showed several tentative high peaks at 36, 59 and 3.6 days.

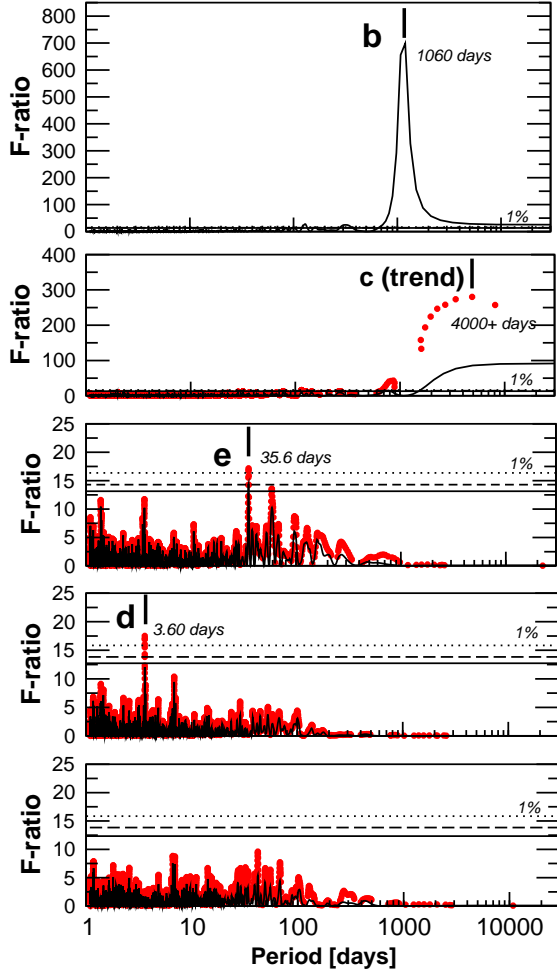


**Fig. 1.** Detection periodograms from most significant signal to less significant one (top to bottom). Black lines are least-squares periodograms computed on the residuals to the k-planet model. The red dots represent the refined orbital solution with k+1-planet as obtained by the recursive periodogram. The resulting sampling of the red dots is not uniform in frequency because the tested k+1 period is also allowed to adjust.

While a solution including the 36 and 3.6 days signals provided a very extreme reduction of the RMS (from 3.1 to 1.6 m s<sup>-1</sup>), the peaks in the periodograms of the residuals provided analytic FAP estimates too large to be acceptable ( $\sim 5\%$ ). A quick-look Bayesian analysis of the same new RVs Tuomi (2012), also indicated that additional candidates were strongly favoured by the data. As we will shown in the analysis section, the RV measurements of GJ 676A are a textbook example where signal correlation prevents the detection of lower amplitude signals using periodogram methods based on the analysis of the residuals only.

## 4. Planetary system : new candidates

### 4.1. Recursive periodogram analysis

For the recursive periodogram analysis, a 1.0 m s<sup>-1</sup> jitter was added in quadrature to the nominal uncertainty of each RV measurement. This value was chosen because, for any multi-planet solution we attempted, about  $\sim 1.0$  m s<sup>-1</sup> always had to be added in quadrature to match the nominal uncertainties to the RMS of the residuals. As seen in the top panel of Figure 1, there

is little doubt on the reality of first already reported candidate (GJ676Ab, Forveille et al. 2011).

Instead of fitting a trend, we performed a recursive periodogram search for a second planet with periods between 1.1 and 50 000 days, obtaining a preferred solution around 4000 days. The presence of a peak at *only* twice the time baseline indicates the presence of significant curvature (see top-left panel in 2). As for GJ 676Ab, there is little doubt on the statistical significance of this signal/trend (analytic FAP threshold of 1% is around 15, while the signal has an F-ratio of several hundreds). As shown in the second panel of Figure 1, the recursive periodogram (red dots) compared to the periodogram on the residuals (black line) is able to massively improve the significance of this second signal thanks to the simultaneous adjustment of the orbit of the first candidate. As discussed in the Bayesian analysis section, the period and parameters of this candidate are not well constrained and only some nominal values are given for reference. For detection purposes only, we conservatively assume that it can be well reproduced by a full Keplerian solution and added it to the model.

After the first two signals were included, the recursive periodogram search for a third companion revealed one additional periodicity at  $\sim 35.5$  days (F-ratio  $\sim 17.5$ ). The analytic FAP was 0.156 %, which warranted the empirical FAP computation. In the first 1000 trials, 5 trials generated false alarms (FAP  $\sim 0.5\%$ ) meaning that more trials are necessary to securely asses if the FAP is  $< 1\%$ . An extended run with  $10^4$  trials produced an empirical FAP of  $\sim 0.44\%$  so the candidate was finally accepted. The candidate (GJ 676Ae) corresponded to a super-Earth/sub-Neptune mass candidate with  $M \sin i \sim 11 M_{\oplus}$ . Even though the preferred eccentricity was rather high ( $\sim 0.6$ ) quasi-circular orbits are still allowed by the data. This candidate would receive  $\sim 2.6$  times more stellar radiation than the Earth receives from the Sun so it would have a hard time keeping oceans of liquid water on its surface (Selsis et al. 2007).

Again, this 35.5 days candidate was included in the models as a third full Keplerian signal and a recursive periodogram search was obtained to look for further companions. A strong isolated peak (F-ratio 19.5, P=3.6 days), was the next promising one signal, showing an analytic FAP as low as 0.015 %. Only 1 test over the first 1000 trials generated a spurious peak with higher power, indicating that the FAP is significantly lower than 1% and the candidate was accepted right away. The new candidate (GJ 676Ad) has a minimum mass of  $\sim 4.5 M_{\oplus}$  and it is certainly too close to the star to support liquid water on its surface.

The recursive periodogram search for a fifth signal show that the next tentative periodicities have analytic FAP at the 10% or higher level, which did not satisfy our preliminary detection criteria so we stopped searching for additional candidates. Even though 4 planet signals might seem a lot given that *only* 75 RVs were used, let us note the the amplitudes of the close-in low mass companions are relatively high (2 – 3 m s<sup>-1</sup>, see Figure 2) compared to the final RMS of the solution (1.6 m s<sup>-1</sup>) and the nominal uncertainties.

### 4.2. Bayesian analysis

As already discussed, there no doubt that RV data of GJ 676A contains the signal of a massive planet ( $m_p = 4.9 M_{\text{Jup}}$ ) with an orbital period of roughly 1060 days (Forveille et al. 2011) and a long period trend. A model with a Keplerian signal and a linear trend was chosen as the starting point of the Bayesian analyses.

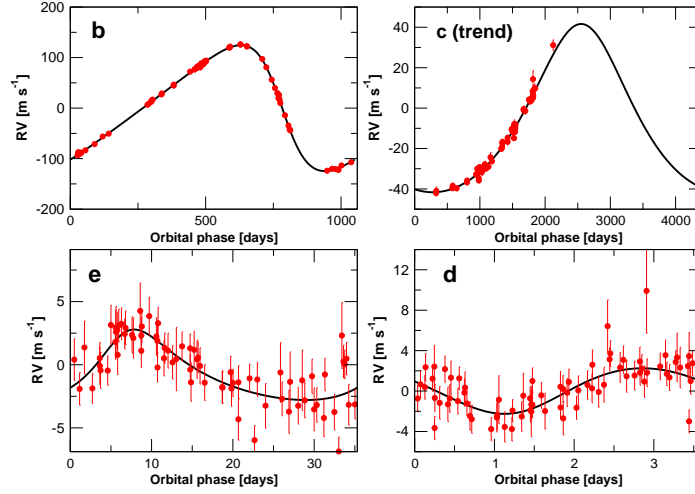


**Fig. 2.** Phase folded radial velocity curves of the reported new planet candidates. Even though curvature is clearly detected (top right panel), the orbit of the of longer period companion is still poorly constrained.

**Table 2.** Relative posterior probabilities of models with  $k = 1, \dots, 4$  Keplerian signals ( $\mathcal{M}_k$ ) with or without a linear trend (LT), the Bayesian evidences  $P(d|\mathcal{M}_k)$ , and RMS values.

$k$	$P(\mathcal{M}_k d)$	$\log P(d \mathcal{M}_k)$	RMS [ms <sup>-1</sup> ]
1+LT	$1.0 \times 10^{-30}$	-224.0	4.59
2	$1.8 \times 10^{-17}$	-192.8	3.00
3	$3.6 \times 10^{-12}$	-179.9	2.20
4	$\sim 1$	-152.9	1.67

While spotting the signature of the massive planet in the RVs was trivial, we observed that instead of a linear trend, the samplings preferred a second Keplerian instead, indicating the presence of significant curvature. Therefore, the second model to be tested contains the trend modeled as a Keplerian. However, because the long-period signal could not be constrained, we fixed its eccentricity and period to their most probable values in the parameter space (for period, this space was the interval between 1 and  $10T_{\text{obs}}$  days, where  $T_{\text{obs}}$  is the baseline of the data) throughout the analyses. Because the orbit is only partially covered by the time-baseline of the observations, we could not constrain its other parameters much either so only the MAP values for this candidate are given in Table 3 as a reference. Fixing period and eccentricity, however, allowed us to draw representative samples from the parameter space and to calculate reliable estimates for the Bayesian evidences of each model. The curvature in the long-period trend was so clearly present in the data that including curvature (through a fixed period-eccentricity Keplerian) increased the model probability by a factor of  $1.8 \times 10^{13}$  and decreased the RMS of the residuals from 4.59 to 3.00 ms<sup>-1</sup> (Table 2).

We continued by adding a third Keplerian signal to the statistical model and performed samplings of the corresponding parameter space. The Markov chains quickly converged to a solution that contained the same periodic signal at 35.4 days also spotted by the recursive periodograms. The model with  $k = 3$  Keplerians was found to have a posterior probability  $2.0 \times 10^5$  times that of a model with  $k = 2$  Keplerians (Table 2). The signal at 35.4 days corresponds to a planet candidate with a minimum mass of 11.5  $M_{\oplus}$ . When sampling the parameter space of a four-Keplerian model, we identified a fourth strong signal in the data with a period of 3.60 days. This was, again, the same 4th period spotted by the recursive periodogram. Our solution of the model

with  $k = 4$  further increased the model probability by a factor of  $2.8 \times 10^{11}$  compared to a model with  $k = 3$ , so we could conclude that this 3.60 day periodicity was also very confidently present in the data (Table 2).

The search for additional periodic signals failed to identify significant periodicities so we conclude that the model probabilities imply the existence of 4 Keplerian signals : the massive companion GJ 676Ab at 1.8 AU; a trend with some curvature suggesting the presence of another massive giant planet in an long period orbit; and two previously unknown planet candidates with orbital periods of 3.60 and 35.4 and minimum masses of 4.4 and 11.5  $M_{\oplus}$  (Table 3; Fig. 2). These signals satisfied all the aforementioned detection criteria as the radial velocity amplitudes were clearly strictly positive and their periods, apart from the long-period signal, were well constrained and had narrow distributions in the parameter space. In addition to the MAP parameter estimates, standard errors, and 99% BCSs in Table 3, we show the distributions of the periods, RV amplitudes, and eccentricities in Fig. 3. These distributions show that – apart from the eccentricities of the two new low-mass companions, that peaked close to zero – all densities were close to Gaussian shape.

#### 4.3. Robustness of the Bayesian solution

To assess the reliability of our solution to the GJ 676A RVs, and indeed that of the Bayesian methods in general in assessing the existence of Keplerian signals in RV data, we performed a test analysis of the first 50 epochs only. The purpose of this test was to investigate whether we could spot the same signals, and receive the same solution from a smaller number of observations. The 50 first epochs have a baseline of approximately 1199 days (roughly two thirds of the full baseline of 1794 days), and because of their lower number, we expected them to constrain the model parameters less, i.e. yielding broader posterior densities, and that the model probabilities are less strongly in favour of – possibly even against – the existence of the two new planet candidates reported in this work.

Again, we started with a model containing a single Keplerian signal and a linear trend. These were easy to spot from the partial RV set and we could identify the same massive planet candidate and trend reported by Forveille et al. (2011, , 69 CCF measurements were used in that work). However, when we sampled the parameter space of a two-Keplerian model, we rapidly



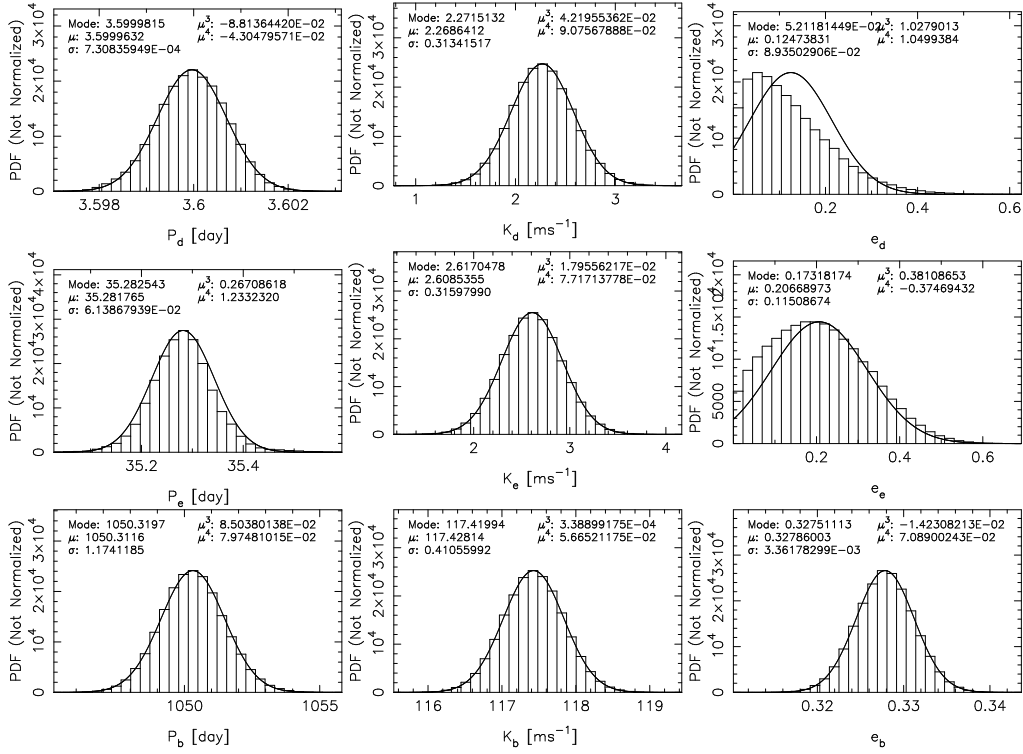


**Fig. 3.** Distributions estimating the posterior densities of orbital periods ( $P_x$ ), radial velocity amplitudes ( $K_x$ ) and eccentricities ( $e_x$ ), and three constrained Keplerian signals. The solid curve is a Gaussian density with the same mean ( $\mu$ ) and variance ( $\sigma^2$ ) as the parameter distribution has. Additional statistics, mode, skewness ( $\mu^3$ ) and kurtosis ( $\mu^4$ ) of the distributions are also shown.

**Table 3.** Orbital solution of the three innermost companions of HD GJ 676A and the excess RV jitter. MAP estimates, the standard errors, and the 99% BCSs.

Parameter	d	e	b	c(trend)*
$P$ [days]	$3.6000 \pm 0.0008$ [3.5978, 3.6022]	$35.37 \pm 0.07$ [35.10, 35.45]	$1050.3 \pm 1.2$ [1046.9, 1053.7]	4400
$e$	$0.15 \pm 0.09$ [0, 0.42]	$0.24 \pm 0.12$ [0, 0.56]	$0.328 \pm 0.004$ [0.318, 0.339]	0.2
$K$ [ $\text{ms}^{-1}$ ]	$2.30 \pm 0.32$ [1.35, 3.19]	$2.62 \pm 0.32$ [1.66, 3.57]	$117.42 \pm 0.42$ [116.18, 118.66]	41
$\omega$ [rad]	$5.5 \pm 1.9$ [0, $2\pi$ ]	$5.8 \pm 2.2$ [0, $2\pi$ ]	$1.525 \pm 0.012$ [1.491, 1.557]	6.21
$M_0$ [rad]	$4.1 \pm 1.7$ [0, $2\pi$ ]	$0.9 \pm 2.0$ [0, $2\pi$ ]	$0.957 \pm 0.036$ [0.844, 1.056]	3.1
$\sigma_j$ [ $\text{ms}^{-1}$ ]	$1.38 \pm 0.18$ [0.95, 1.97]			
Derived parameters				
$a$ [AU]	$0.0413 \pm 0.0014$ [0.037, 0.045]	$0.187 \pm 0.007$ [0.17, 0.21]	$1.80 \pm 0.07$ [1.62, 1.99]	5.2
$m_p \sin i$ [ $M_\oplus$ ]	$4.4 \pm 0.7$ [2.4, 6.4]	$11.5 \pm 1.5$ [6.5, 15.1]	$1570 \pm 100$ [1190, 1770]	951
$m_p \sin i$ [ $M_{\text{jup}}$ ]	$0.014 \pm 0.002$	$0.036 \pm 0.005$	$4.95 \pm 0.31$	3.0
$S/S_0^\dagger$	48.1	2.3	0.025	0.003

**Notes.** (\*) Since all parameters are poorly constrained, the the MAP solution is provided for orientative purposes only.

(†) Stellar irradiance  $S$  at the planet's orbit divided by the flux received by the Earth from the Sun ( $S_0$ ).

discovered another Keplerian signal at 35.5 day period. The corresponding two-Keplerian solution together with the linear trend increased the posterior probability of the model by a factor of  $1.0 \times 10^4$ , which clearly exceeded the detection threshold of 150. Furthermore, we also identified a third periodicity at 3.60 days when increasing the complexity of the statistical model by adding another Keplerian signal to it. This model was  $5.0 \times 10^5$  times more probable than the model with  $k = 2$ , so we could conclude that, three planet candidates and a linear trend were already strongly suggested by these initial 50 RVs. Moreover, the two new low-amplitude periodic signals satisfy our detection criteria by having amplitudes strictly above zero ( $2.27$  [ $1.00$ ,  $3.41$ ]  $\text{ms}^{-1}$  and  $2.83$  [ $1.48$ ,  $4.04$ ]  $\text{ms}^{-1}$  for GJ 676A e and d, respectively) and well constrained orbital periods ( $3.6000$  [ $3.5963$ ,

$3.6027$ ] days and  $35.48$  [ $35.16$ ,  $35.90$ ] days, respectively). This solution is consistent with the one received for the full data set in Table 3, which implies that the two new planets could already have been detected in the HARPS RVs when the 50th spectrum was obtained back in October 2009, possibly even earlier.

We performed the recursive periodogram analysis on the same 50 epochs. Again, the massive GJ 676Ab and the trend were also trivially. Then we attempted a recursive periodogram search for a third Keplerian. This search spotted the 35.5 days signal as the next most likely periodicity, but provided an analytic FAP of 15 % which did not satisfy our preliminary detection criteria (analytic FAP > 1%). In order to check if the 3.6 days candidate could be inferred by periodogram methods, we added the 35.5 days signal to the model and performed a recursive pe-

riodogram search for a fourth candidate. Although a peak at 3.6 days peak was present, it was not, by far, the most significant periodicity suggested by the recursive periodogram.

This result implies that Bayesian methods are clearly more sensitive in detecting low-amplitude signals compared to classic periodogram approaches (even compared to our newly developed recursive periodogram method). Even if a researcher prefers to obtain frequentist confirmation (e.g., empirical FAP) of a signal before announcing it, early Bayesian detections can be used to optimize observational strategies and sample the periods of interest. We are conducting simulations with synthetic dataset to identify failure modes of the proposed Bayesian methods (e.g., identify situations that could generate false positives) and refine the detection criteria accordingly.

## 5. Conclusions

We re-derived high precision radial velocities on the public HARPS observations of GJ 676A using our newly developed HARPS-TERRA software, obtaining a significant improvement over the RVs obtained using the CCF approach. We developed a recursive periodogram method to enhance the sensitivity of least-squares solvers to low amplitude signals in the presence of strong multiplanet correlations and provide a recipe to derive empirical FAPs. We compare the results obtained on the RV of GJ 676A to the candidates identified by a Bayesian analysis obtaining compatible detection of the same four signals. We provide the favoured 4 planet solution together with the allowed parameter intervals as derived from the Bayesian MCMC samplings.

While it is clear that Bayesian methods are more general and provide a more complete description of the data, frequentists methods (e.g., empirical FAP computations) allow a simpler interpretation of the significance of a detection. The combination of criteria from both approaches provides great confidence in our results. We have shown that after the early Bayesian detection of 4 planets, 25 more measurements we sufficient to confirm the same candidates with periodogram based methods. Even if a researcher prefers frequentist confirmation of candidates, early Bayesian detection can be used to optimize follow-up programs (Gregory 2005). In overview, we have shown that the confluence of recent data analysis developments (HARPS-TERRA, Bayesian toolbox, advanced periodograms) achieve a significant boost in sensitivity to very low-mass companions in existing datasets. Compared to the significant investment done in hardware development, development of more optimal data-analysis methods comes at a significantly lower cost thus enabling a more efficient utilization of the observational resources.

Concerning the new two planet candidates, we find that they are both in the sub-Neptune mass regime. The shorter period candidate (GJ 676Ad) has a significant probability of transit ( $\sim 5\%$  according to Charbonneau et al. 2007) thus encouraging the photometric follow-up of the star. The presence of a long period companion (massive planet or a brown dwarf) is now obviously detected through significant curvature in the trend and a period of  $\sim 4000$  days or longer is preliminary suggested by the data. After GJ 876 (Rivera et al. 2010) and GJ 581 (Mayor et al. 2009), GJ 676A becomes the third M dwarf with 4 planet candidates. Except for the Solar system itself, this planetary system has the broadest range of minimum masses and periods reported so far (from  $5 M_{\oplus}$  to  $5 M_{Jup}$ , and from 3.6 days to 4000 or more days). Despite of the abundance of candidates, the periods (and corresponding semi-major axis) are spaced enough that we do not anticipate major dynamical stability issues. Compared to the

more dynamically packed GJ 581 and GJ 876 systems, the orbits of the candidate planets leave ample room to detect further potential candidates in intermediate orbits whenever additional RV observations become available. Due to the proximity of GJ 676A to our Sun ( $\sim 16.4$  pc), the long period, massive candidates are attractive targets for direct imaging attempts (Lagrange et al. 2010). Given that the make-up of stars in binary systems should be similar, it would be very interesting to investigate whether GJ 676B (M3.5V) has been as prolific as GJ 676A in forming all kinds of planets.

*Acknowledgements.* GAE is supported by the German Federal Ministry of Education and Research under 05A11MG3. M. Tuomi is supported by RoPACS (Rocky Planets Around Cools Stars), a Marie Curie Initial Training Network funded by the European Commission's Seventh Framework Programme. We are grateful for the advice, support and useful discussions obtained from Paul Butler (DTM), Ansgar Reiners (IAG), Mathias Zechmeister (AIG) and Hugh Jones (HU). We thank Sandy Keiser for setting up and managing the computing resources available at the Department of Terrestrial Magnetism–Carnegie Institution of Washington. This work is based on data obtained from the ESO Science Archive Facility under request number GANGLFGGCE178541. This research has made extensive use of the SIMBAD database, operated at CDS, Strasbourg, France; and the NASA's Astrophysics Data System.

## GJ 676A

## References

- Anglada-Escudé, G., Arriagada, P., Vogt, S. S., et al. 2012, *ApJ*, 751, L16
- Anglada-Escudé, G. & Butler, R. P. 2012, *ApJS*, 200, 15
- Anglada-Escudé, G., López-Morales, M., & Chambers, J. E. 2010, *ApJ*, 709, 168
- Baliunas, S. L., Donahue, R. A., Soon, W. H., et al. 1995, *ApJ*, 438, 269
- Baranne, A., Queloz, D., Mayor, M., et al. 1996, *A&AS*, 119, 373
- Bonfils, X., Delfosse, X., Udry, & et al. 2011, e-prints arXiv:1111.5019
- Butler, R. P., Marcy, G. W., Williams, E., et al. 1996, *PASP*, 108, 500
- Charbonneau, D., Brown, T. M., Burrows, A., & Laughlin, G. 2007, *Protostars and Planets V*, 701
- Chib, S. & Jeliazkov, I. 2001, *J. Am. Stat. Ass.*, 96, 270
- Cumming, A. 2004, *MNRAS*, 354, 1165
- Delfosse, X., Forveille, T., Ségransan, D., et al. 2000, *A&A*, 364, 217
- Forveille, T., Bonfils, X., Lo Curto, G., et al. 2011, *A&A*, 526, A141+
- Gomes da Silva, J., Santos, N. C., Bonfils, X., et al. 2012, eprint arXiv:1202.1564
- Gregory, P. C. 2005, *ApJ*, 631, 1198
- Haario, H., Saksman, E., & Tamminen, J. 2001, *Bernoulli*, 7, 223
- Johnson, J. A. & Apps, K. 2009, *ApJ*, 699, 933
- Kass, R. E. & Raftery, A. E. 1995, *J. Am. Stat. Ass.*, 90, 773
- Koen, C., Killick, D., van Wyk, F., & Marang, F. 2010, *MNRAS*, 403, 1949
- Lagrange, A.-M., Bonnefoy, M., Chauvin, G., et al. 2010, *Science*, 329, 57
- Levenberg, K. 1944, *Quarterly of Applied Mathematics*, 2, 164
- Lovis, C., Dumusque, X., Santos, N. C., et al. 2011a, *ArXiv e-prints*
- Lovis, C., Ségransan, D., Mayor, M., et al. 2011b, *A&A*, 528, A112
- Mayor, M., Bonfils, X., Forveille, T., et al. 2009, *A&A*, 507, 487
- Mayor, M., Marmier, M., Lovis, C., et al. 2011, *ArXiv e-prints*
- Pepe, F., Lovis, C., Ségransan, D., et al. 2011, *A&A*, 534, A58+
- Pepe, F., Mayor, M., Galland, & et al. 2002, *A&A*, 388, 632
- Pepe, F., Rupprecht, G., Avila, G., & et al. 2003, in *SPIE Conference Series*, Vol. 4841, 1045–1056
- Press, W. H., Teukolsky, S. A., Vetterling, W. T., & Flannery, B. P. 1992, *Numerical recipes in FORTRAN. The art of scientific computing* (Cambridge: University Press, —c1992, 2nd ed.)
- Queloz, D. 1995, in *IAU Symposium*, Vol. 167, *New Developments in Array Technology and Applications*, ed. A. G. D. Philip, K. Janes, & A. R. Upgren, 221
- Queloz, D., Henry, G. W., Sivan, J. P., et al. 2001, *A&A*, 379, 279
- Rivera, E. J., Laughlin, G., Butler, R. P., et al. 2010, *ApJ*, 719, 890
- Scargle, J. D. 1982, *ApJ*, 263, 835
- Selsis, F., Kasting, J. F., Levrard, B., & et al. 2007, *A&A*, 476, 1373
- Skrutskie, M. F., Cutri, R. M., Stiening, R., et al. 2006, *AJ*, 131, 1163
- Tuomi, M. 2011, *A&A*, 528, L5
- Tuomi, M. 2012, *A&A* accepted, arXiv:1204.1254
- Tuomi, M. & Kotiranta, S. 2009, *A&A*, 496, L13
- Tuomi, M., Pinfield, D., & Jones, H. R. A. 2011, *A&A*, 532, A116
- van Leeuwen, F. 2007, *A&A*, 474, 653
- Wilken, T., Lo Curto, G., & Probst, R. e. a. 2012, *Nature*, 485, 611



Wright, J. T. & Howard, A. W. 2009, *ApJS*, 182, 205

Zechmeister, M., Kürster, M., & Endl, M. 2009, *A&A*, 505, 859

**Table 4.** Differential HARPS-TERRA RV measurements of GJ 676A measured in the Solar System Barycenter reference frame. Secular acceleration has been subtracted to the RVs.

BJD (days)	RV (m s <sup>-1</sup> )	$\sigma_{RV}$ (m s <sup>-1</sup> )
2453917.74799	-49.64	1.07
2453919.73517	-42.40	1.74
2454167.89785	50.99	0.87
2454169.89585	47.69	0.74
2454171.90444	51.41	0.76
2454232.81801	50.43	0.82
2454391.49180	-112.11	0.83
2454393.48993	-116.14	0.85
2454529.90084	-192.95	1.02
2454547.91501	-190.21	0.82
2454559.81569	-182.54	1.10
2454569.90363	-189.17	1.31
2454571.88945	-190.03	0.58
2454582.82029	-181.49	0.82
2454618.75558	-173.61	1.27
2454658.69933	-156.68	0.73
2454660.66163	-150.04	0.95
2454661.77222	-151.70	0.65
2454662.67523	-154.15	1.01
2454663.81158	-150.58	0.99
2454664.79004	-147.60	1.11
2454665.78637	-152.21	0.78
2454666.69605	-153.22	0.65
2454670.67260	-151.17	1.13
2454671.60332	-150.03	1.01
2454687.56195	-149.86	0.98
2454721.55487	-133.47	1.11
2454751.49069	-117.35	2.14
2454773.50237	-108.57	0.87
2454916.81980	-44.78	0.60
2454921.89297	-48.26	0.99
2454930.90684	-40.74	0.95
2454931.79510	-40.19	0.91
2454935.81778	-39.01	0.52
2455013.68661	1.94	1.01
2455013.74372	0.0	1.18
2455074.52005	25.37	0.81
2455090.50702	31.96	0.95
2455091.52880	30.62	2.30
2455098.49414	31.37	0.42
2455100.54094	36.65	0.51
2455101.49047	33.88	0.91
2455102.50286	32.35	1.46
2455104.54025	35.68	0.89
2455105.52363	34.53	2.14
2455106.51997	35.83	1.05
2455111.50933	35.28	0.55
2455113.49787	38.06	0.57
2455115.51499	43.93	1.84
2455116.48753	38.80	0.64
2455117.49304	44.05	1.01
2455121.52664	49.34	1.23
2455122.50532	47.43	0.87
2455124.49783	46.58	0.56
2455127.51679	47.31	0.53
2455128.51395	51.17	0.53
2455129.49540	50.53	0.70
2455132.49575	50.21	0.74
2455133.49318	49.77	0.77
2455259.90727	90.78	1.19
2455260.86440	90.78	0.79
2455284.89313	84.51	1.37
2455340.70850	67.31	1.06
2455355.79544	50.55	0.94
2455375.61072	25.37	1.11
2455387.65668	10.96	1.39
2455396.53797	0.18	1.31
2455400.64286	-8.10	0.58
2455401.59478	-5.14	0.95
2455402.59092	4.03	4.06
2455404.64556	-9.17	1.97
2455407.57676	16.70	0.67